

Removal of Microplastics and Performance of a Developed Ceramic Filter



Natália Vogel , Matheus Felipe Pedrotti , André Zimmer* 

Federal Institute of Education, Science, and Technology of Rio Grande do Sul, Feliz Campus

ABSTRACT: The consumption of microplastics can have harmful effects. To effectively remove microplastics from water using an affordable device, this study developed a ceramic filter based on clay and waste glass. The research evaluated the addition of a porogenic agent and the effects of firing temperature. In the formulations, clay was substituted by a porogenic agent with 10 and 20 by weight, maintaining 10 by weight of waste glass. Ceramic filters were produced by molding press, and evaluated for their physical properties. Its performance was assessed by water permeability at different pressures, leaching of elements, and removal of microplastics. As a result, formulations with a higher porogenic agent content and lower firing temperature present superior permeability, however, permeability increases after higher pressure tests, when structure fracture may occur. Moreover, the formulation with the lowest porosity (without adding a porogenic agent) achieved an impressive removal rate of nearly 99.8%. It was concluded that a ceramic filter could retain microplastics well, as long as the filtration pressure and porosity were optimized to obtain the best results – higher filtration without fracture.

Keywords: ceramic, filter, performance, microplastic, removal, porosity

1. INTRODUCTION

Over the years, the production of plastic has grown, and it is currently the material most used by human beings [1]. In 2021, world production was 390 million tons of this material [2], and Brazil is the fourth country that produces the most plastic waste in the world, which is 10,675,989 tons [3].

Plastic pollution influences soil, air, and water quality [4]. Because of this, concerns have been raised about the presence of plastics in the marine environment, which now numbers around 50-75 trillion in the ocean [5], and takes hundreds of years to degrade. The presence of this material generates environmental impacts such as the death of fish, mammals, and seabirds, as well as the destruction of the ecosystem [6], Plastic can also be broken down into microplastics, which are insoluble in water and reach dimensions of between 1 and 1000 μm [1], according to the ISO/TR 21960/2020 standard, and are conducive to the adherence of organic pollutants [6].

According to Vethaak and Legler [7], microplastics when ingested or inhaled by humans, potentially reach various organs, where they may cause health issues by damaging cells and triggering inflammatory and immune responses. Li et al. [8] review the effects of microplastics when studied through experimental models, organoids, and animals. Their findings indicate that microplastics can cause oxidative stress, DNA damage, organ dysfunction, metabolic disorders, immune system responses, neurotoxicity, and reproductive and developmental toxicity.

A study [9] about carotid artery plaque found that 58.4% of investigated patients with the presence of microplastics and nanoplastics, which is associated with a risk of cardiovascular disease of myocardial infarction, stroke, or death from any cause, being a hazard ratio of 4.53 higher than whom these substances were not detected.

Therefore, it is necessary to find solutions to remove microplastics from water through water treatment [4, 10]. To retain microplastics, coagulation, and sedimentation techniques have been studied, and shown to be effective in removing large particles between 15 and 140 μm in size, but with an efficiency of 33% for particles as small as 10 μm , which also go through the subsequent stage of sand filtration [4].

Filtration represents a barrier to suspended solids in water and is an effective process against turbidity, coloration, and microorganisms, where retention will depend on the characteristics of the filter medium and the flow rate [11]. Thinking of a simple and low-cost device for removing impurities that remain suspended in water, there is the ceramic filter, used to retain microorganisms and any other small particles. The ceramic filter is a technique used in water treatment in which, through filtration, water passes through a porous ceramic medium [12, 13].

Received : August 27, 2024

Revised : September 25, 2024

Accepted : October 01, 2024

Ceramic filters [14] and membranes [15] effectively trap particles from water due to their fine pores. However, fouling remains an unavoidable challenge for ceramic membranes, leading to decreased flow rates and necessitating frequent cleaning [16, 17]. In contrast, ceramic filters offer an extended lifespan facilitated by their easy maintenance; they can be periodically washed and reused [18]. Moreover, they present a cost-effective alternative to membranes, boasting a lower initial investment [17].

The ceramic filters commonly were made from a mixture of clay and porogenic agent, where a wet mixture passes through a forming process to obtain different shapes, such as a disk, candle, pot, and tube. After forming, the samples were dried followed by firing in a kiln [19]. In the firing process, the porogenic agent is commonly used to generate pores, which are the means of filtering water [20–22]. Several porogenic agents have already been used in the production of ceramic filters, including sawdust [12, 13, 23], wood flakes [24], and rice husks [25, 26], among others.

A porogenic agent already studied in a ceramic matrix to control porosity is yerba mate waste [27]. This material is processed from the leaves and stems of the *ilex paraguariensis* plant and is used to prepare a drink known as "mate", or "chimarrão". This drink is consumed socially in countries such as Argentina, Brazil, Uruguay, Paraguay, and Chile. In Brazil, it is widely consumed in the state of Rio Grande do Sul [28, 29], being a waste after consumption [27].

Because yerba mate as a porogenic agent increases the porosity of the ceramic material, it consequently reduces its mechanical strength [27]. Thus, the inclusion of waste glass could improve the cohesion of particles from the ceramic matrix, due to its chemical composition, consisting mainly of silica, calcium oxide, and sodium oxide, which the last acts as a strong flux, contributing to sinterization for more resistance of ceramic filter. In addition, its incorporation into ceramic formulation lowers the firing temperature, reducing energy consumption [30, 31].

The current strategy focuses on producing a ceramic filter using affordable local materials, including clay, glass waste, and yerba mate waste as a porogenic agent, to evaluate microplastic filtration in water. Additionally, the present study examines the balance between porosity, filtration efficiency, microplastic removal, flow rate, leaching, and mechanical integrity under pressure in ceramic filters, as these factors have not been thoroughly addressed in existing research.

2. METHODS

2.1 Raw Materials and Formulations

The ceramic filters were produced from three formulations prepared, where the contents of the glass waste had maintained constant, and clay had successively substituted by yerba mate, as shown in Table 1.

During the ceramic firing process, the particles of raw materials undergo coalescence in a process known as sintering. As the temperature and time increase, porosity reduces because the coalescence rises, which reduces the

permeability of sintered samples.

Clay could be fired in temperatures in the order of 900 °C to produce ceramic parts. In an investigation [32] for clay application, the addition of waste glass significantly enhanced the sintering process, leading to improved strength characteristics, where the waste glass was incorporated into brick clay at ratios of 0% (reference), 2.5%, 5%, and 10%, and the samples were fired at temperatures of 850, 950, and 1050 °C.

The formulations presented in Table 1 include waste glass to reduce the sintering temperature and facilitate glass recycling. A porogenic agent is necessary to enhance porosity, which promotes filtration. Clay is the primary constituent due to its suitable properties for processing ceramic products, such as filters, resulting in an inert material.

The clay selected had a raw material used for the production of bricks and had been tested in a previous investigation that had presented its characteristics, such as composition, phases, and particle size distribution [33]. Discarded amber container glass was used as waste glass, a material that had demonstrated a uniform composition of soda-lime-silica glass [34]. Yerba mate after infusion in a drink called *chimarrão* was used as a porogenic agent because of its high decomposition at temperatures below 550 °C, as it had resulted in total ashes between 5.5 and 6.2% [35].

The percentages used were defined based on previous tests, taking into account that the percentages of 0, 10, and 20% yerba mate had been studied by Scharnberg et al. [27], and the content of waste glass was kept at 10% which had shown better results when added to ceramic material [36].

Waste glass and clay had dried at 105 °C and the yerba mate at 45 °C, both in a Med Clave model 5 oven. After, the yerba mate was ground in a Solab SL-31 knife mill and sieved through a 60-mesh sieve with an aperture of 250 µm. The rest of the yerba mate that had remained on the sieve had ground again and the process had repeated until total sieving. The clay and waste glass had been ground in a Servitech CT-12058 hammer mill.

Table 1 Formulations with the amounts of raw materials used (% by mass - wt. %).

| Formulation | Clay | Yerba mate | Waste glass |
|-------------|------|------------|-------------|
| 9C1G | 90 | 0 | 10 |
| 8C1G1Y | 80 | 10 | 10 |
| 7C1G2Y | 70 | 20 | 10 |

2.2 Preparation of the Specimens

The clay, yerba mate, and waste glass were weighed and the raw materials were added to a BP Engenharia CB2-T eccentric mill, where they were grounded/mixed for 15 minutes. Then 8% water (by mass) was added and mixed manually. The formulations were then placed in a hermetic container for 24 hours.

After this process, the material was pressed in a hydraulic press (Mawil machine, 15-ton model) and circular samples with a diameter of 50 mm were produced to evaluate the ceramic filter performance, and rectangular samples with dimensions of 76 x 36 mm, to measure its physical properties. A pressure of 20 MPa was applied to form the test specimens.

Following, the samples were left at room temperature (~20 °C) for 24 hours and then placed in an oven at 110 °C until they had completely dried when they had sintered in a Jung model 24010 muffle furnace at temperatures of 900 and 950 °C, using a heating rate of 1.6 °C/min and a plateau of 5 min. The temperatures utilized were established based on previous studies, including Hasan et al. [37], whom examined clay brick incorporating waste glass (2 - 40 wt.%), and Scharnberg et al. [27], whom investigated ceramic formulations made from clay, waste glass, and yerba mate.

Table 2 shows the number of samples for each formulation for the tests. Samples were prepared in triplicate for each test, totaling 144 rectangular samples and 60 circular samples. For the leaching and microplastic removal tests, only samples sintered at the temperature that showed the best flow results were used. The results are shown as the average of the values obtained and the standard deviation.

Table 2 Number of sample prepared for each formulation

| Test | Shape | Number of specimens | | |
|---|-------------|---------------------|--------|---------|
| | | 900 °C | 950 °C | Unfired |
| Loss of ignition and firing shrinkage | Rectangular | 9 | 9 | - |
| Water absorption, apparent porosity, and apparent density | Rectangular | 6 | 6 | - |
| Flexural strength | Rectangular | 6 | 6 | 6 |
| Optical microscopy | Circular | 1 | 1 | - |
| Mass flow rate | Circular | 6 | 6 | - |
| Cycle of pressure versus mass flow | Circular | 2 | - | - |
| Leaching | Circular | 2 | - | - |
| Microplastic removal | Circular | 2 | - | - |

2.3 Assessment of Processes and Products

The samples evaluated for loss on ignition and firing shrinkage were weighed and measured before and after the firing process, and the values were calculated using Equations 1 (loss on ignition) and 2 (shrinkage):

$$LOI = \frac{M_d - M_f}{M_d} \times 100 \tag{1}$$

$$S = \frac{L_i - L_f}{L_i} \times 100 \tag{2}$$

Where:

LOI = loss of ignition (%)

M_d = dry mass (g)

M_f = mass after firing (g)

S = shrinkage (%)

L_i = initial length (mm)

L_f = final length (mm)

For the water absorption, apparent density, and apparent porosity tests, the ABNT NBR ISO 10545/3 standard had followed - Ceramic Slabs - Part 3: Determination of water absorption, apparent porosity, relative density, and apparent density. The samples were dried in an oven at 110 °C until completely dry. The samples were then weighed. The material was then immersed in water for 24 hours and weighed again to determine its suspended mass.

After impregnation, the samples were wiped dry with a microfiber cloth and weighed again to obtain the wet mass. Using these values, water absorption (Equation 3), apparent density (Equation 4), and apparent porosity (Equation 5) were calculated.

$$WA = \frac{M_f - M_d}{M_d} \times 100 \tag{3}$$

$$AD = \frac{M_d}{M_f - M_i} \times 100 \tag{4}$$

$$AP = \frac{M_f - M_d}{M_f - M_i} \times 100 \tag{5}$$

Where:

WA = water absorption (%)

AD = apparent density (g/cm³)

DP = apparent porosity (%)

M_d = dry mass (g)

M_f = mass after firing (g)

M_i = impregnated suspended mass (g)

The flexural strength was assessed using a three-point fleximeter at 4.2 mm/s on the specimens. The distance between the support bars was 49 mm. With these values, the flexural strength was determined using Equation 6:

$$FS = \frac{3Fl}{2bh^2} \tag{6}$$

Where:

FS = flexural strength (N/mm²)

F = breaking load (N)

l = distance between support bars (mm)

b = smaller side of the specimen (mm)

h = minimum specimen thickness (mm)

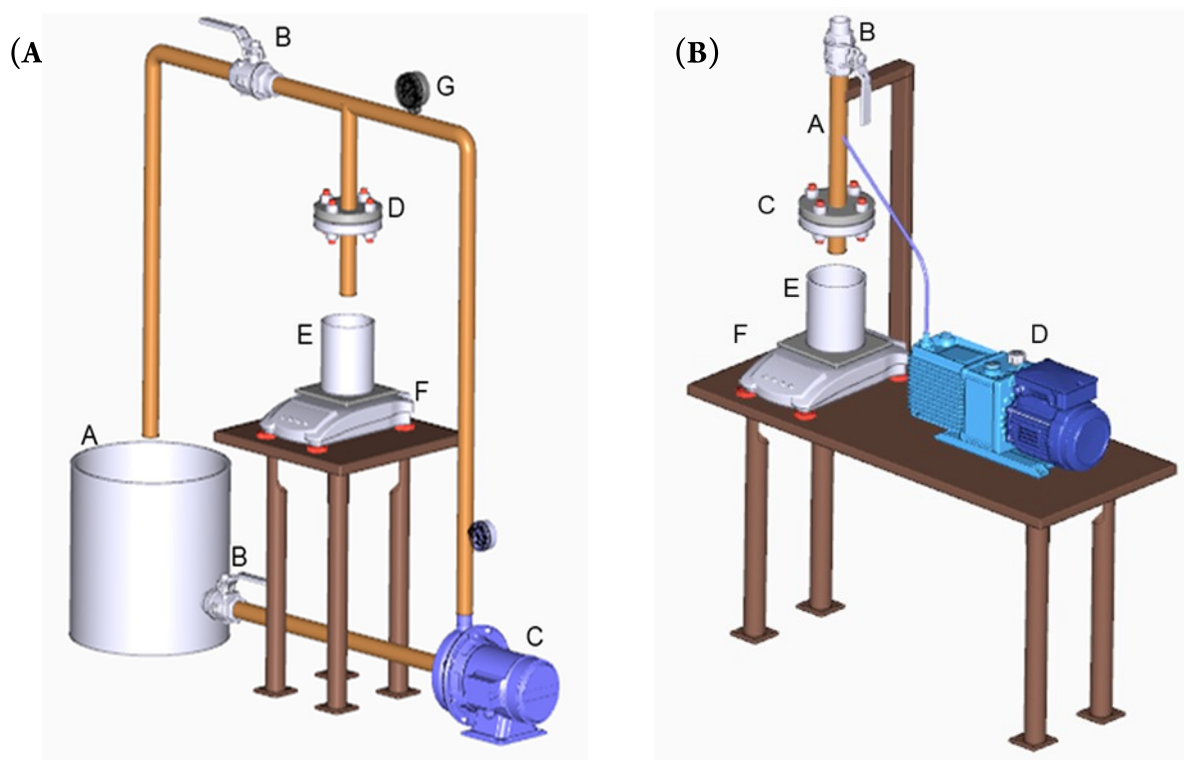


Fig. 1. Systems developed to (A)¹ measure flow into the filters; and (B)² evaluate leaching. Legend: ¹ A = storage tank, B = register, C = hydraulic pump, D = support containing the ceramic filter, E = container for collecting water, F = balance, and B = pressure gauge. ² A = System containing tube, B = register, C = support containing the ceramic filter, D = air compressor, E = water collection container, and F = balance.

The surface of the specimens was also analyzed using a Physis brand optical microscope at 50x magnification to visualize the structure of the ceramic filters.

2.4 Developed Apparatus to Evaluate Ceramic Filters

To assess the flow of fluid through the filters produced, the system shown in Figure 1A was developed, to test the mass flow by applying pressure values of 0, 50, 100, 150, and 200 kPa, and Figure 1B shows the apparatus developed to evaluate microplastic removal as to check for leaching of the elements sodium and potassium that might be present in the ceramic filter, applying a fixed pressure value of 100 kPa. For the flow test tap water was used, while distilled water was used for leaching and microplastic removal tests.

2.5 Fluid Flow Through Ceramic Filters

In the system shown in Figure 1A, where pressure difference values (ΔP) were applied and maintained at 0, 50, and 100 kPa for the 7C1G2Y formulation, collecting water for 3 min. For the 8C1G1Y formulation, water was collected for 5 min, and for the 9C1G every 10 min, both at pressures of 50, 100, 150, and 200 kPa. The difference in collecting water time was for maintaining a similar total fluid mass passed through the filters developed. Thus, for each pressure applied, the mass collected was checked and the mass flow rate was calculated using Equation 7.

$$m = \frac{m}{t} \quad (7)$$

Where:

m = mass flow rate (g/s)

m = mass (g)

t = time (s)

Based on this test, and to identify whether there were variations in the flow of water through the samples due to changes in the structure of the material, such as an increase in pores or breaks, an experiment of a cycle of pressure versus mass flow was carried out. A cycle of the fluid pressure increasing (0 to 200 kPa) and decreasing (200 to 0 kPa) was applied to see if there were any changes in the flow rate.

2.6 Leaching

In the system shown in Figure 1B, 50 mL of distilled water was added, this being the maximum volume of the tube (A), the air compressor (D) had turned on at a fixed pressure of 100 kPa, and the volume of 50 mL water had passed through. Only in formulation 7C1G2Y, to see if there was any difference in the leaching of the components, the filtration of 50 mL was repeated three times for the same specimen, totaling 150 mL of water collected.

The leaching tests attempted to identify the presence of the element's sodium and potassium in the filtrate and their relative measurements were made using a model 910M atomic emission photometer from Analyzer, using the emission lines of 588 nm for sodium and 766.5 nm for potassium.

2.7 Removal of Microplastics

To retain microplastics present in water in the ceramic filters developed, a suspension was synthesized in the laboratory from polystyrene (PS) plastic, which had been chosen because of its rigidity and higher density than water – the first able it to ground at micro-scale and the second to disperse it in water. The plastic had broken up with a hammer and ground in a Solab SL-31 knife mill. It was then ground for two hours in the BP Engenharia CB2-T eccentric mill and sieved through a 325-mesh sieve with an aperture of 45 μm .

To obtain the suspension, 0.2 g of microplastics were mixed in 400 mL of distilled water, and for better dispersion of the sample, it was placed in an ultrasound tank (Cristófoli model 2.5 L) at a frequency of 42 kHz until it had completely dispersed - about 30 min.

Various techniques have been employed to detect its removal: Berov and Klayn [38] utilized an Olympus SZ51 stereomicroscope with SZ2-ILST support, van der Hal et al. [39] employed a Motic SMZ171 stereomicroscope, Xu et al. [40] used micro-Fourier transform infrared spectroscopy (μ -FT-IR) with a Bruker LUMOS, and Nie et al. [41] conducted micro-Raman spectroscopy using a Thermo Fisher Scientific DXR2.

Its removal efficiency can also be measured using turbidity, which is considered a simple and inexpensive method [4, 42]. The concentration of the dispersion is a function of turbidity, i.e. a change in concentration can influence turbidity over time [43]. This can be exemplified by the dispersion of polystyrene particles larger than 50 μm , which caused a decrease in the turbidity of aqueous dispersions [4]. Thus, the turbidity of the suspensions was

then measured using a model HI 98703 portable turbidimeter from Hanna Instruments.

A 50 mL of the suspension was placed in the system shown in Figure 1B and a pressure of 100 kPa was applied, where the sample was collected and its turbidity was measured before and after the test, and the removal efficiency was calculated using Equation 8. The mass flow rate during the passage of the suspension containing microplastics was also calculated using Equation 8.

$$RE = \frac{T_i - T_f}{T_i} \times 100 \quad (8)$$

Where:

RE = removal efficiency (%)

T_i = initial turbidity (NTU)

T_f = final turbidity (NTU)

3. RESULTS

3.1 Processing and Ceramic Filter Characteristics

The ceramic filters developed in this work are shown in Figure 2. It can be seen they present a reddish color because the clay used is rich in iron oxides.

It was also found that the 7C1G2Y formulations were thicker than the others, reaching 9 mm, against 7 mm for the 9C1G and 8 mm for the 8C1G1Y formulations. This difference was probably related to the packing of the particles [30] since the used volume in the mold cavity had been kept constant for the different formulations. It is convenient to lower thickness as the porogenic agent reduces or is absent at formulations to favor flow through the ceramic filter.

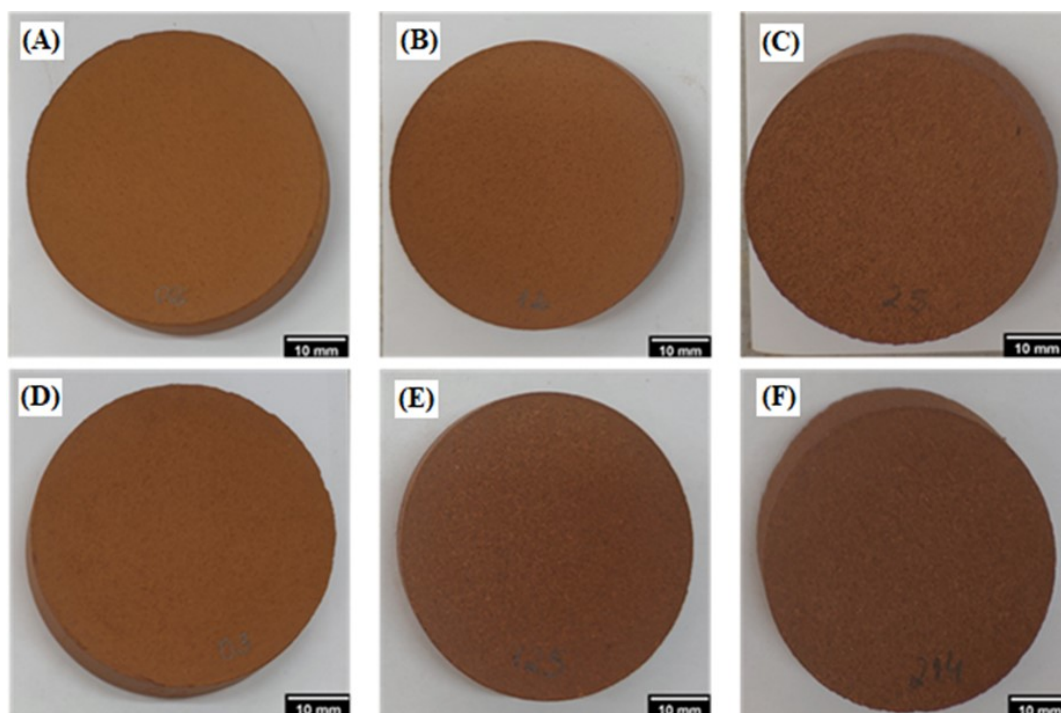


Fig. 2. Images of developed ceramic filters after a firing cycle of 900 °C: (A) 9C1G; (B) 8C1G1Y; (C) 7C1G2Y; and at 950 °C: (D) 9C1G; (E) 8C1G1Y; and (F) 7C1G2Y.

Figure 3A shows that LOI increased as the yerba mate content in the formulations increased. During the sintering of the specimens [27] the yerba suffered degradation of its principal constituents - cellulose, hemicellulose, and lignin [29]. It is still necessary to consider that the clay interfered due to the decomposition of its possible constituents like carbonates, sulfides, hydrated oxides, organic matter, and the dehydroxylation of clay minerals, all of which interfered with the weight loss during the firing process [44]. Despite soda-lime-silica glass, which is produced at temperatures above 1600 °C, it is not expected that there will be a loss of mass of this component at temperatures of 900 and 950 °C.

The firing shrinkage is presented in Figure 3B where could be noted that higher temperature (950 °C) was the principal factor influencing their values, not demonstrating differences between formulations at the same temperatures.

Scharnberg et al. [27] studied firing shrinkage for formulations similar to the one used in this work, where they maintained 20 wt.% of glass in the formulations, modifying the yerba mate and clay contents. From this, they observed an increase in firing shrinkage both for the addition of glass and yerba mate waste and for the increase in temperature, finding values of 0.3 to 2.3% for samples fired at 900 °C, and 3.0 to 6.1% for samples fired at 1100 °C. They also found that as the yerba mate content increased, there was an increase in firing shrinkage, due to the sintering evolution as the temperature increased.

It can be seen that the 7C1G2Y formulations had higher apparent porosity values, and it can be supposed that yerba mate was the main factor behind this increase since it was predominantly organic, as shown in Figure 3A. This fact was also verified by Yakub et al. [45] who obtained from formulations of ceramic filters produced with sawdust, a

porosity between 36 and 48%.

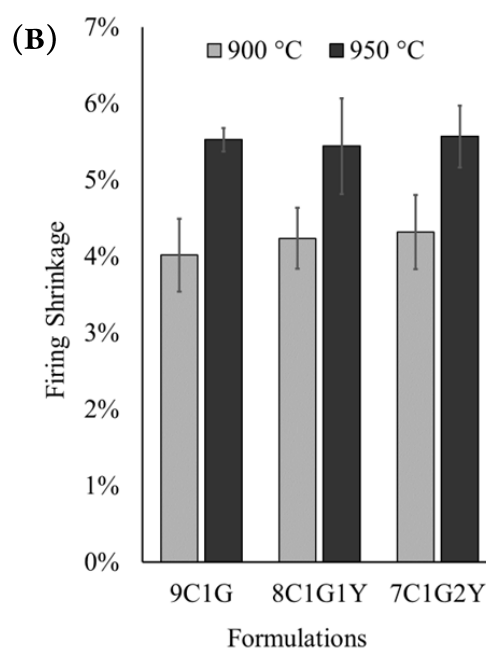
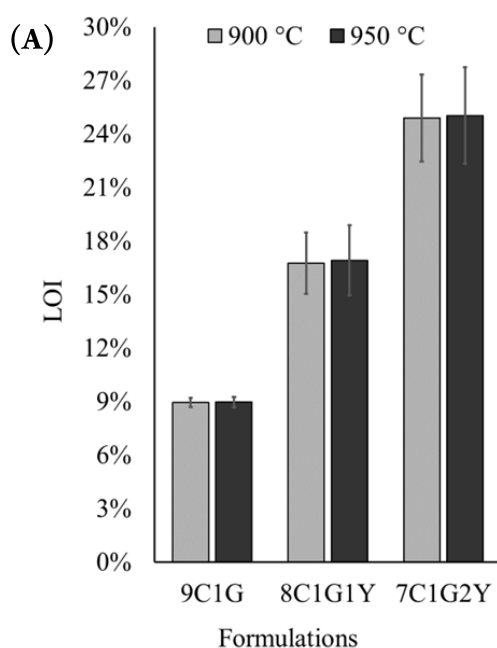
Apparent porosity has also been studied in previous studies for different types of porogenic agents, as can be seen in Table 3.

Table 3 Apparent porosity of ceramic filters found for different porogenic agents.

| Porogenic agent | Wt. % of porogenic agents | Firing temperature (°C) | Porosity (%) | Reference |
|---|----------------------------------|-------------------------|--------------|-----------------------|
| Sawdust | 25 | 700 | 63.91 | [13] |
| Rice husk | 35 | 1000 | 56.60 | [25] |
| Cornstarch ¹ and sludge ² | 5 ¹ + 85 ² | 950 | 64.60 | [46] |
| Yerba-mate | 20 | 900 | 48.42 | Present investigation |

Studies from Bulta and Micheal [13] and Dung et al. [25] showed higher porosity results when compared to the respective work, possibly because they used a different forming process, as well as a higher porogenic agent content Mouratib et al. [46] achieved greater porosity than the other studies using 5% of corn starch and 85% of water treatment sludge, both porogenic agent, despite their organic and degradable principal constituents.

As apparent porosity increases (Figure 3C), the apparent density decreases (Figure 3D). There was also a



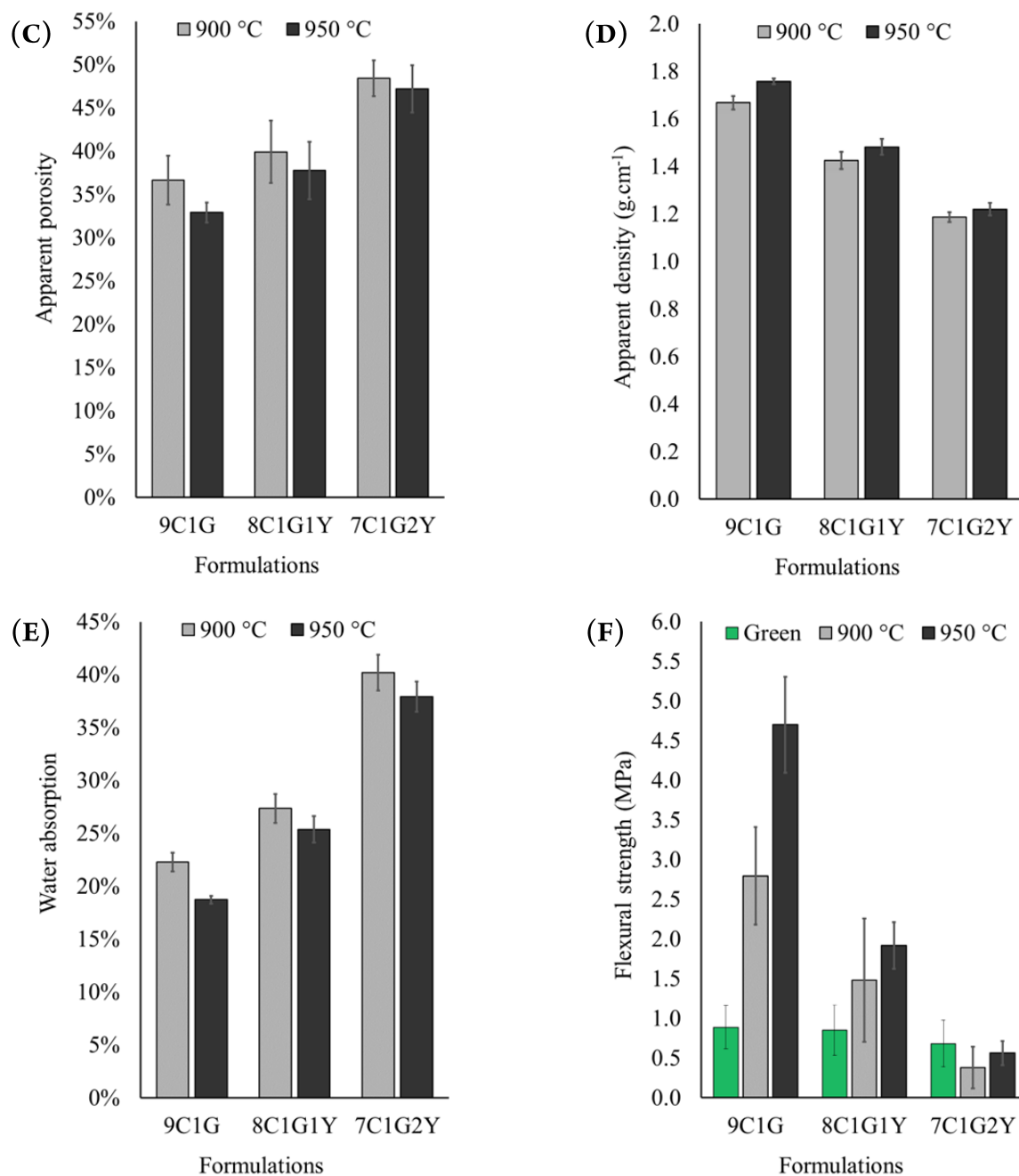


Fig. 3. Ceramic filter properties after 900 and 950 °C firing cycles: (A) loss on ignition; (B) firing shrinkage; (C) apparent porosity; (D) apparent density; (E) water absorption; and (F) flexural strength.

slight variation in density when the material was sintered at a higher temperature, that is when this increase occurs, the liquid phase is formed, causing it to permeate the spaces between the particles present in the ceramic structure [47]. In addition, firing at a higher temperature presents more sinterization which results in greater firing shrinkage, resulting in a material with a higher apparent density and lower porosity [25].

The fact that the material has greater porosity also affects its water absorption, as can be seen in Figure 3E. The same was found by Bohn et al.[30], who studied the insertion of waste glass in ceramic tiles, and also found a reduction in water absorption as the firing temperature

increased. This reduction occurs due to the sintering of the material, and is more intense despite the formation of a glassy phase, reducing porosity and interfering with water absorption [27, 30].

This behavior was also found in the work of Scharnberg et al. [27], who evaluated the addition of waste glass and yerba mate in a ceramic matrix, that is, with the increase in the yerba mate content, there was an increase in water absorption. Similar results were also found by Mustapha et al. [48] for the manufacture of ceramic vessel filters consisting of kaolin and sawdust, and as the last one increases in the formulation, the greater the water absorption.

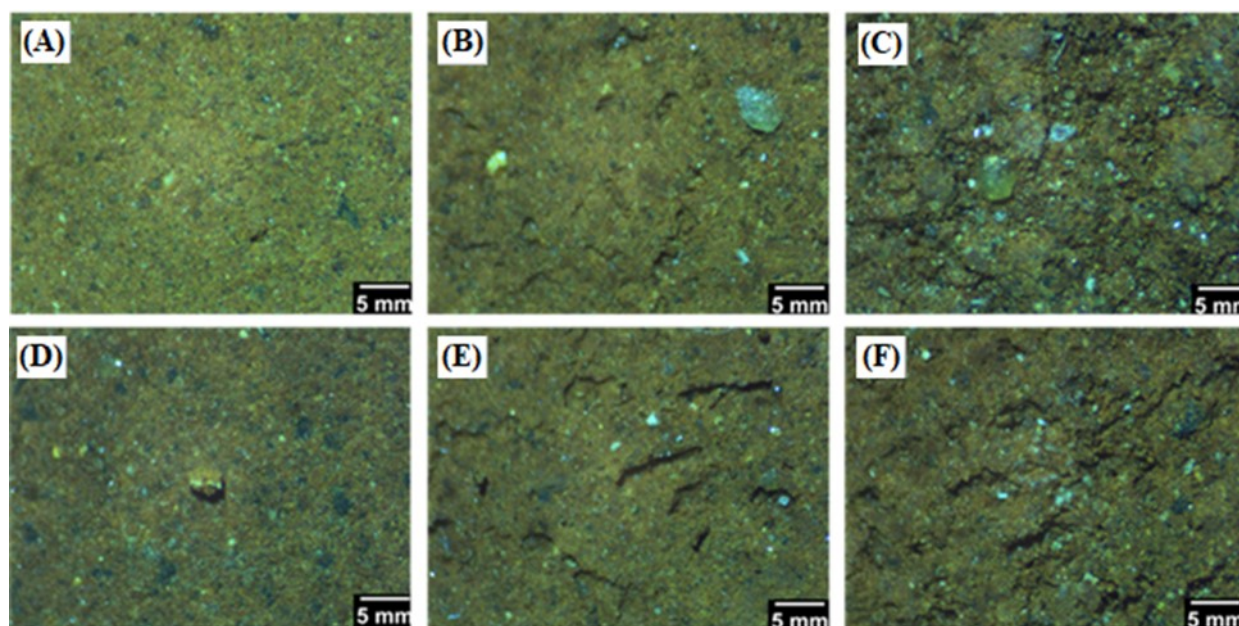


Fig. 4. Microscopic image of the samples firing at 900 °C: (A) 9C1G; (B) 8C1G1Y; (C) 7C1G2Y; and at 950 °C: (D) 9C1G; (E) 8C1G1Y; and (F) 7C1G1Y.

As the porosity of the material increased, its mechanical strength decreased, as shown in the results obtained from the flexural strength from Figure 3F. This fact is attributed because pores could be understood as a void or absence of material from sectional area under loading, reducing then the total material that supports the load, also around the pore's surface the load concentrates stress, and both were the main reasons for the taking out mechanical strength.

The unfired specimens (or green samples) from all formulations present similar flexural strengths to each other (Figure 3F). Malik et al. [49] found that with a greater presence of clay in the manufacture of specimens, greater resistance was achieved. It is known that clay is the principal raw material responsible for unfired properties, which reveals that yerba mate practically does not influence this property.

The formulations sintered at higher temperatures at 950 °C achieved superior flexural strength (Figure 3F), reaching 4.70 MPa in the 9C1G formulation. The formulations containing a higher yerba mate content showed greater porosity (Figure 3D), and consequently, there was less resistance in these formulations (Figure 3F).

Mouratib et al. [46] presented similar results and defined that with an increase in flexural strength, there is less apparent porosity. In addition, mechanical strength values of 11.59 to 24.06 MPa were found when the firing temperature had increased from 950 to 1150 °C, demonstrating the effect of sintering on the material. This can also be seen in the respective work, in which the strengths were higher in the formulations that went through the firing process. Scharnberg et al. [27] stated that as flexural strength decreased, water absorption increased, with values ranging from 0.5 to 20 MPa. The highest strength value was achieved for the formulation containing 20% waste glass and sintered

at 1100 °C. Certainly, because they used a higher firing temperature than in the respective work, there was greater sintering, increasing its mechanical strength. In both studies like the present study, mechanical strength decreased as the amount of yerba mate added increased.

The surficial structure of the ceramic filters was checked using optical microscopy, obtaining the images shown in Figure 4. Visually there were fewer pores in the 9C1G formulation (Figure 4E), as the porogenic agent increases in the formulation, a greater presence of pores with elongated and irregular shapes occurs (Figure 4A, B, C).

Similar results were found by Scharnberg et al. [27], who found interconnected pores at 900 °C and closed pores at 1100 °C due to better sintering of the glass waste present, justifying better uniformity in the structure of the samples and resulting in better mechanical properties.

3.2 Fluid Flow Through Ceramic Filters

Figure 5A, B indicates that the 9C1G and 8C1G1Y formulations showed slight variation in terms of mass flow rate when the same air pressure value was applied. However, the 7C1G2Y formulation showed a higher mass flow rate than the others, due to its higher apparent porosity (Figure 3C). The apparent porosity also interfered with results according to the pressure applied, where specimen from formulation 7C1G2Y caused damage above the pressure of 100 kPa, as well as easy fluid passage through this specimen with only water column pressure (10 cm), different from the other formulations.

When comparing the same formulations at different firing temperatures, there was no significant difference for the 9C1G formulation, but there was a small increase in flow rate for the 8C1G1Y formulation at 200 kPa. The same was found for the 7C1G2Y formulation, showing a higher mass flow rate at a firing temperature of 900 °C (Figure 5A).

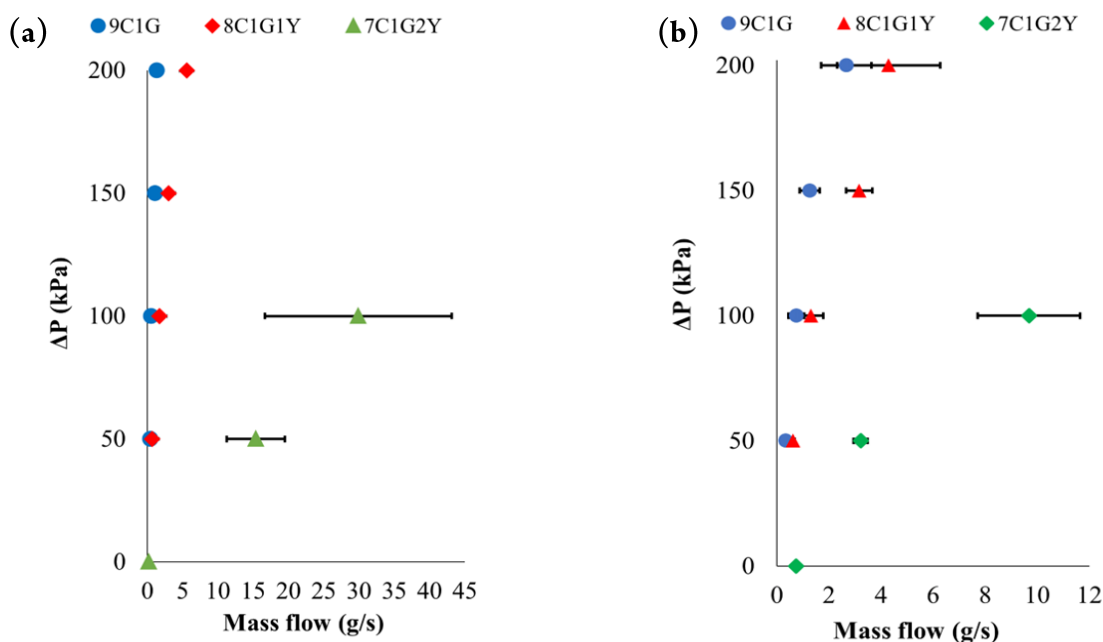


Fig. 5. Mass flow rates of formulations sintered at (a) 900 °C*; and (b) 950 °C. *Some results have a minimal standard deviation.

According to Figure 3C, the formulations sintered at 900 °C had superior apparent porosity than those sintered at 950 °C, which could explain the higher flow rate when the same pressure value was applied.

The permeation flux of ceramic filters with different porogenic agents was studied for coconut husk and eggshell [50], corn starch [46], and graphite [51]. The results are shown in Table 4 and compared to the present study, in which could be observed that when none or low pressure was applied, the permeation flux was between 0.145 and 3.68 mL.cm⁻².min⁻¹ since the amount of porosity varies from 31.20 to 56.8%. When pressures were applied to filtration, the present work demonstrates that there was possibly a considerable increase in the permeation flux, in height as 142.60 mL.cm⁻².min⁻¹.

This difference in flow may be related to the network structure of the pore generated in the material, which can be classified as open (interconnected), closed (isolated or connected only with neighboring cells), blind (with no outlet), or mixed porosity, in addition to being structured in an aligned or leveled manner [52]. Open porosity, i.e., with interconnected pores, is advantageous for transporting fluids, as in the case of filtration, and closed porosity is favorable for thermal insulation [53].

An experiment was carried out to see if fractures occurred in the ceramic filter structure when fluid pressure was applied. A cycle of increasing and decreasing pressure was then applied to check for changes in flow rate. Figure 6 shows hysteresis in this test in the formulations 8C1G1Y and 7C1G2Y, those that contain a porogenic agent. On the opposite the formulation without a porogenic agent (9C1Y) when a cycle of increase and decrease of pressure does not reveal hysteresis (Figure 6).

According to Figure 6, the most porous formulation (7C1G2Y) had a significant water mass flow without applying pressure, maintaining the water column constant. With 150 kPa of pressure applied, the ceramic filter from this formulation broke. Thus, confirming that pressure applied to the ceramic filter could damage its internal structure, facilitating the flow. As the porosity amount increases, the finer the structure unifying parts inside the filter, which could be damaged under pressure resulting in an easier fluid flow.

3.3 Leaching

Since yerba mate generates ash after the ceramic firing process [29, 54], containing elements that could solubilize and leach during the passage of water through the filter, the leaching test was carried out on the 9C1G, 8C1G1Y, and 7C1G2Y formulations sintered at a lower temperature (900 °C), lesser sintered and then more susceptible for leaching.

Sodium and potassium elements had leached during the passage of water through the ceramic filter (Table 5). As used clay, an aluminosilicate, which its chemical composition consists of SiO₂ (48.6%), Al₂O₃ (17.9%), Fe₂O₃ (16.7%) with little sodium and potassium ions, present at Na₂O (0.58%) and K₂O (1.19%) [33], but it is possible to leach these elements. Yerba mate, on the other hand, can contain sodium and potassium [55], which can vary depending on its cultivation and infusion temperature [56, 57], but are easily extracted through the infusion process [58]. Because yerba mate used here is after its infusion, there was expected little presence of these elements. Therefore, as the glass waste contains higher concentrations of CaO, MgO, K₂O, and Na₂O [30, 36], it is considered that its presence interfered with the increase in sodium and potassium elements.

Table 4 Permeation flux in ceramic filters composed of different porogenic agents

| Porogenic agent | Wt. % of porogenic agent | Firing temperature (°C) | Porosity (%) | Flux (mL.cm ⁻² .min ⁻¹) | Pressure applied (kPa) | Reference |
|---------------------------|--------------------------|-------------------------|--------------|--|------------------------|-----------------------|
| Coconut husk and eggshell | 25 | 1000 | 31.20 | 3.5 | 20 | [50] |
| | 0 | 950 | 32.91 | 12.74 | 200 | |
| Corn starch | 5 | 1050 | 46.70 | 0.145 | 12 | [46] |
| Graphite | 30 | 1350 | 56.8 | 3.68 | none | [51] |
| | 10 | 950 | 37.75 | 26.70 | 200 | |
| Yerba-mate | 20 | 900 | 48.42 | 142.60 | 100 | Present investigation |
| | 20 | 900 | 48.42 | 3.56 | none | |

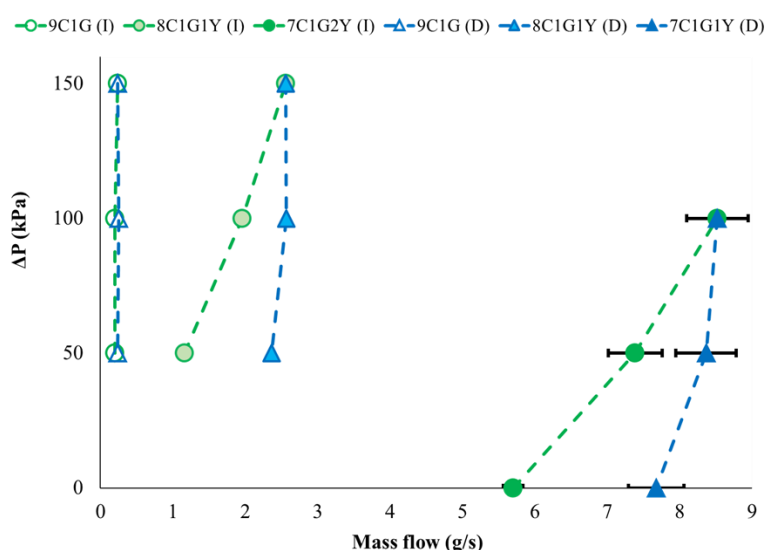


Fig. 6. Cycle of pressure versus mass flow carried out on the 9C1G, 8C1G1Y, and 7C1G2Y formulations sintered at 900 °C, applying increased (I) and decreased (D) pressures of 50, 100 and 150 kPa. *Specimens 9C1G and 8C1G1Y have minimal standard deviation in mass flow results.

The leaching of elements from the passage of water through ceramic filters was also verified in the work by Matthies et al. [59]. They studied leaching from ceramic filters produced in Indonesia and made from local clay mixed with rice husks. The results showed leaching of elements such as arsenic, manganese, and silver, with values of 0.09 mg/L, 0.2 mg/L, and 0.01-0.03 mg/L being found in the filtrate, respectively. According to the authors, the concentration of the elements manganese and silver was below the WHO (World Health Organization) limits, but arsenic was above the limit of 0.01 mg/L, requiring 33.5 L of water to pass through the filter to achieve leaching below this value. The arsenic probably came from the clay but may have been the result of the rice husk used as a porogenic agent, as this element can be present in the soil or contaminated water [59].

Table 5 Leaching relative measurements found for the elements sodium and potassium in water filtered through the 9C1G, 8C1G1Y, and 7C1G2Y formulations sintered at 900 °C.

| Formulation | Volume filtered (mL) | Sodium (mg/L) | Potassium (mg/L) |
|-------------|----------------------|---------------|------------------|
| 9C1G | 50 | 0.300 ± 0.015 | 0.020 ± 0.001 |
| 8C1G1Y | 50 | 0.012 ± 0.006 | < LOD |
| | 50 | 0.090 ± 0.005 | < LOD |
| 7C1G2Y | 100 (2 x 50) | 0.020 ± 0.001 | < LOD |
| | 150 (3 x 50) | < LOD | < LOD |

3.4 Removal of Microplastics

Fig. 3C demonstrates the presence of porous in developed filters, which enables water to flow through while trapping the microplastics (filtration). The microplastics dispersed in water after passing through the ceramic filters developed presented high filtration (removal) of microplastics by comparing the initial and final turbidity measured in the test realized, as pointed out by removal efficiency presented in Table 6.

Table 6 Microplastic removal efficiency of sintered formulations at 900 °C, applying pressure of 100 kPa.

| Formulation | Initial turbidity (NTU) | Final turbidity (NTU) | Efficiency (%) |
|-------------|-------------------------|-----------------------|----------------|
| 9C1G | 305 ± 15.25 | 0.71 ± 0.035 | 99.77 ± 0.199 |
| 8C1G1Y | 305 ± 15.25 | 3.03 ± 0.151 | 99.01 ± 0.182 |
| 7C1G2Y | 305 ± 15.25 | 8.38 ± 0.419 | 97.30 ± 0.146 |

The turbidity of the suspension decreased after passing through the ceramic filters, and the less porous the filter, the greater the removal of microplastics. This relationship between porosity and turbidity removal efficiency was also verified by Bulta and Micheal [13] who evaluated the turbidity of river water samples in ceramic filters made from clay and sawdust, where the results of the turbidity removal efficiency ranged from 31.11 to 82.11%, and the clay and sawdust content varied, affecting the porosity of the material. Thus, increasing the sawdust content led to an increase in porosity and a reduction in turbidity removal efficiency, in the same way as in the present study.

The evaluation of turbidity was also carried out by Bolaji and Akande [23] on ceramic filters made of clay and

sawdust with silver applied to their surface. The filtered samples were raw water from a well, rain, river, and artesian well, and the results for turbidity efficiency were 94.4, 89.4, 97.2, and 91.3 %, respectively.

Porosity plays a key role in the relationship between flow rate and the removal of microplastics from water using ceramic filters. Lower porosity demonstrated greater efficiency in retaining microplastics, effectively capturing these particles, while higher porosity resulted in less effective filtration. Therefore, incorporating yerba mate to create pores was essential for improving water flow through the ceramic filter. A formulation containing 20 wt.% yerba mate achieved a microplastic removal efficiency exceeding 97% (Table 6), enabling the filter to operate effectively without the need for applied pressure (Fig. 6).

3.5 Mass Flow Rate of a Suspension with Microplastic

The mass flow rate versus time during the filtration test is shown in Figure 7. The formulation 9C1G, lesser porous, took appreciably more time to filter at 100 kPa, 50 mL of microplastic suspension, compared to the others. On the opposing side, the highest porosity of formulation 7C1G2Y caused on mass flow rate an increase followed by a decrease, this is attributed to the changes during filtration, initially because of some collapse from more fragile porous regions followed by a cake formation, which increased resistance of flow.

For the 9C1G formulation, the mass flow rate was practically constant, while for 8C1G1Y there was a decrease in flow rate attributable to the formation of cake on the surface of the filter. It was also found that the 9C1G formulation had a lower mass flow rate compared to the others, as well as a longer test time, both accredited by its lowest porosity compared to other formulations (Figure 3C).

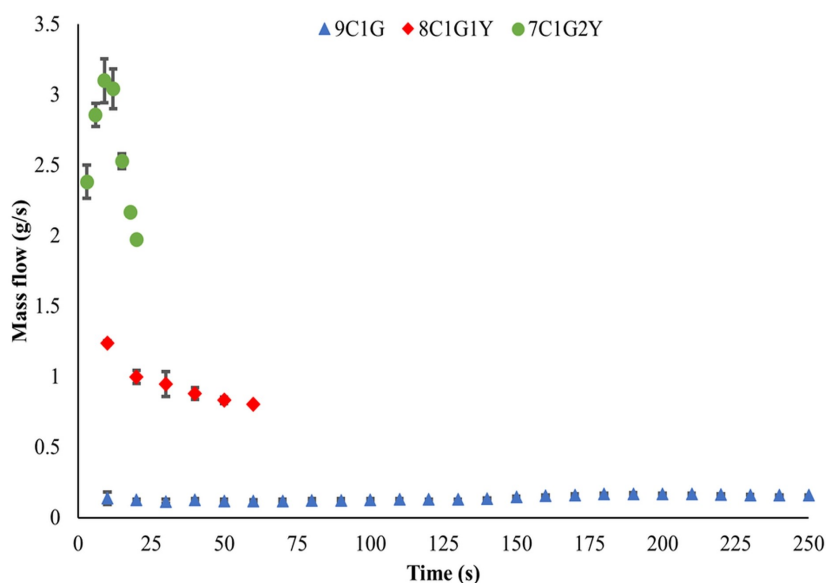


Fig. 7. Mass flow rates during time obtained for the 9C1G, 8C1G1Y, and 7C1G2Y formulations, sintered at 900 °C, after passing the suspension containing microplastics, applying a pressure of 100 KPa. *Some results have a minimal standard deviation.

4. SUMMARY

A simple ceramic filter based on clay and waste glass could reach adequate results for the removal of microplastics. Adding a porogenic agent based on the yerba mate plant increases the porosity of developed ceramic filters, which makes it possible to more flux with a slight reduction of microplastic removal efficiency.

Depending on the application, principally when requiring a higher filtration rate, or lower time of filtration, higher pressure is necessary to be applied on filtration and this could cause damage to the structure of a more porous filter.

The developed ceramic filter could leach some elements, like sodium and potassium, that occur only on initial filtration. As clay and waste glass have both cited elements in their composition, they were responsible for some leaching.

During the filtration of water with microplastics there was a cake formation, which increases the resistance of permeation of water.

Based on the results could be inferred that as higher the porosity in the ceramic filter, the better will be the permeation flux, but some internal collapse structure could occur, once porosity reduces the area that supports the load.

Further investigations are necessary to optimize ceramic filters when applied pressure - in terms of porosity and mechanical resistance, as well as the formation of cake and its influence in the removal of microplastics, i.e., an optimized process to reach more adequate filtration and resistance.

AUTHOR INFORMATION

Corresponding Author

*Email: andre.zimmer@feliz.ifrs.edu.br

ORCID

Natália Vogel : 0009-0001-5566-1231
 Matheus Felipe Pedrotti : 0000-0002-3492-7686
 André Zimmer : 0000-0003-1520-923X

REFERENCES

- [1] Kye, H., Kim, J., Ju, S., Lee, J., Lim, C., Yoon, Y.: Microplastics in water systems: A review of their impacts on the environment and their potential hazards. *Heliyon*. 9, 1–30 (2023). <https://doi.org/10.1016/j.heliyon.2023.e14359>
- [2] Plastics Europe: Plastics – the Facts 2022, https://plasticseurope.org/wp-content/uploads/2023/03/PE-PLASTICS-THE-FACTS_FINAL_DIGITAL-1.pdf
- [3] World Population Review: Plastic Pollution by Country 2024, <https://worldpopulationreview.com/country-rankings/plastic-pollution-by-country>
- [4] Bayarkhuu, B., Byun, J.: Optimization of coagulation and sedimentation conditions by turbidity measurement for nano- and microplastic removal. *Chemosphere*. 306, 1–9 (2022). <https://doi.org/10.1016/j.chemosphere.2022.135572>
- [5] Fava, M.: Ocean plastic pollution an overview: data and statistics, <https://oceanliteracy.unesco.org/plastic-pollution-ocean/>
- [6] Cole, M., Lindeque, P., Halsband, C., Galloway, T.S.: Microplastics as contaminants in the marine environment: A review. *Mar Pollut Bull.* 62, 2588–2597 (2011). <https://doi.org/10.1016/j.marpolbul.2011.09.025>
- [7] Vethaak, A.D., Legler, J.: Microplastics and human health. *Science* (1979). 371, 672–674 (2021)
- [8] Li, Y., Tao, L., Wang, Q., Wang, F., Li, G., Song, M.: Potential Health Impact of Microplastics: A Review of Environmental Distribution, Human Exposure, and Toxic Effects, (2023)
- [9] Marfella, R., Prattichizzo, F., Sardu, C., Fulgenzi, G., Graciotti, L., Spadoni, T., D’Onofrio, N., Scisciola, L., La Grotta, R., Frigé, C., Pellegrini, V., Muncinò, M., Siniscalchi, M., Spinetti, F., Vigliotti, G., Vecchione, C., Carrizzo, A., Accarino, G., Squillante, A., Spaziano, G., Mirra, D., Esposito, R., Altieri, S., Falco, G., Fenti, A., Galoppo, S., Canzano, S., Sasso, F.C., Matacchione, G., Olivieri, F., Ferraraccio, F., Panarese, I., Paolisso, P., Barbato, E., Lubritto, C., Balestrieri, M.L., Mauro, C., Caballero, A.E., Rajagopalan, S., Ceriello, A., D’Agostino, B., Iovino, P., Paolisso, G.: Microplastics and nanoplastics in atheromas and cardiovascular events. *N Engl J Med.* 390, 900–910 (2024). <https://doi.org/10.1056/NEJMoa2309822>
- [10] Tang, K.H.D., Hadibarata, T.: Microplastics removal through water treatment plants: Its feasibility, efficiency, future prospects and enhancement by proper waste management. *Environmental Challenges*. 5, 1–12 (2021). <https://doi.org/10.1016/j.envc.2021.100264>
- [11] Cescon, A., Jiang, J.Q.: Filtration process and alternative filter media material in water treatment. *Water* (Switzerland). 12, (2020). <https://doi.org/10.3390/w12123377>
- [12] Zereffa, E.A., Bekalo, T.B.: Clay ceramic filter for water treatment. *Materials Science and Applied Chemistry*. 34, 69–74 (2017). <https://doi.org/10.1515/msac-2017-0011>
- [13] Bulta, A.L., Micheal, G.A.W.: Evaluation of the efficiency of ceramic filters for water treatment in Kambata Tabaro zone, southern Ethiopia. *Environmental Systems Research*. 8, 1–15 (2019). <https://doi.org/10.1186/s40068-018-0129-6>
- [14] Erhuanga, E., Banda, M.M., Kiakubu, D., Kashim, I.B., Ogunjobi, B., Jurji, Z., Ayoola, I., Soboyejo, W.: Potential of ceramic and biosand water filters as low-cost point-of-use water treatment options for household use in nigeria. *Journal of Water Sanitation and Hygiene for Development*. 11, 126–140 (2021). <https://doi.org/10.2166/washdev.2020.096>
- [15] Cevallos-Mendoza, J., Amorim, C.G., Rodríguez-Díaz, J.M., Montenegro, M. da C.B.S.M.: Removal of Contaminants from Water by Membrane Filtration: A Review, (2022)

- [16] Alsawafah, N., Abuwatfa, W., Darwish, N., Husseini, G.: A comprehensive review on membrane fouling: Mathematical modelling, prediction, diagnosis, and mitigation, (2021)
- [17] Shafiquzzaman, M., Al-Mahmud, A., Al-Saleem, S., Haider, H.: Application of a low cost ceramic filter for recycling sand filter backwash water. *Water (Switzerland)*. 10, (2018). <https://doi.org/10.3390/w10020150>
- [18] Yang, H., Xu, S., Chitwood, D.E., Wang, Y.: Ceramic water filter for point-of-use water treatment in developing countries: Principles, challenges and opportunities, (2020)
- [19] Venis, R.A., Basu, O.D.: Mechanisms and efficacy of disinfection in ceramic water filters: A critical review. *Crit Rev Environ Sci Technol*. 51, 2934–2974 (2021). <https://doi.org/10.1080/10643389.2020.1806685>
- [20] Heylen, C., Annan, E., Monahan, K., String, G., Lantagne, D.: Modeling of hydraulic performance in disks and full-scale ceramic water filters. *Environ Sci Technol*. 55, 7702–7710 (2021). <https://doi.org/10.1021/acs.est.1c01886>
- [21] Venis, R.A., Basu, O.D.: Mechanisms and efficacy of disinfection in ceramic water filters: A critical review. *Crit Rev Environ Sci Technol*. 51, 2934–2974 (2021). <https://doi.org/10.1080/10643389.2020.1806685>
- [22] Nigay, P.-M., Nzihou, A., White, C., Soboyejo, W., White, C.E., Soboyejo, W.O.: Removal mechanisms of contaminants in ceramic water filters. *Journal of Environmental Engineering*. 144, (2018). [https://doi.org/10.1061/\(ASCE\)EE.1943-7870.0001471i](https://doi.org/10.1061/(ASCE)EE.1943-7870.0001471i)
- [23] Bolaji, B.O., Akande, O.O.: Development and performance evaluation of a ceramic filter for point-of-use water purification. *Analele Universității Eftimie Murgu*. XX, 301–312 (2013)
- [24] Chung, D.H.: Introducing efficient low cost smoked pots for water purification for developing countries. *Journal of Waste Water Treatment & Analysis*. 4, 1–5 (2013). <https://doi.org/10.4172/2157-7587.1000152>
- [25] Dung, T.T.N., Nam, V.N., Nhan, T.T., Hoang, B.N., Hung, D.L.T., Quang, D.V.: Utilization of rice husk, an abundant and inexpensive biomass in porous ceramic membrane preparation: A crucial role of firing temperature. *J Nanomater*. 2021, 1–7 (2021). <https://doi.org/10.1155/2021/8688238>
- [26] Oyanedel-Craver, V.A., Smith, J.A.: Sustainable colloidal-silver-impregnated ceramic filter for point-of-use water treatment. *Environ Sci Technol*. 42, 927–933 (2008). <https://doi.org/10.1021/es071268u>
- [27] Scharnberg, A.R.A., Preibbnow, A. V., Arcaro, S., da Silva, R.M., dos Santos, P.A.M., Basegio, T.M., Rodriguez, A.A.L.: Evaluation of the addition of soda-lime glass and yerba mate wastes in ceramic matrix. *Ceramica*. 65, 63–69 (2019). <https://doi.org/10.1590/0366-69132019653732466>
- [28] Burris, K.P., Harte, F.M., Davidson, P.M., Stewart, C.N., Zivanovic, S.: Composition and bioactive properties of yerba mate (*Ilex paraguariensis* A. St.-Hil.): A review. *Chil J Agric Res*. 72, 268–274 (2012). <https://doi.org/10.4067/S0718-58392012000200016>
- [29] Neves, R.M., Dall Agnol, L., Ornaghi Jr., H.L.: A survey of thermal degradation behavior based on chemical composition of post-consumed coffee and yerba mate. *Cellulose Chemistry and Technology*. 55, 355–363 (2021). <https://doi.org/10.35812/CelluloseChemTechnol.2021.55.34>
- [30] Bohn, B.P., Von Mühlen, C., Pedrotti, M.F., Zimmer, A.: A novel method to produce a ceramic paver recycling waste glass. *Clean Eng Technol*. 2, 1–12 (2021). <https://doi.org/10.1016/j.clet.2021.100043>
- [31] Cruz, R.T. da, Pedrassani, J., Bragança, S.R.: Faianças, grês e porcelanas. *Científika* (2022)
- [32] Demir, I.: Reuse of waste glass in building brick production. *Waste Management and Research*. 27, 572–577 (2009). <https://doi.org/10.1177/0734242X08096528>
- [33] de Almeida, E.M., Mota, J.D., Menegolla, C., Piovesan, M.A., Müller, C., Zimmer, A., Korf, E.P.: Use of sludge from the vehicle industry and its encapsulation of toxic metals in ceramic products. *Environ Sci Pollut Res Int*. 30, 116325–116335 (2023). <https://doi.org/10.1007/s11356-023-30669-4>
- [34] Zimmer, A., Bragança, S.R.: A review of waste glass as a raw material for whitewares. *J Environ Manage*. 244, 161–171 (2019). <https://doi.org/10.1016/j.jenvman.2019.05.038>
- [35] Rossi, G.B., Lozano, V.A.: Simultaneous determination of quality parameters in yerba mate (*Ilex paraguariensis*) samples by application of near-infrared (NIR) spectroscopy and partial least squares (PLS). *LWT - Food Science and Technology*. 126, 1–5 (2020). <https://doi.org/10.1016/j.lwt.2020.109290>
- [36] Phonphuak, N., Kanyakam, S., Chindaprasirt, P.: Utilization of waste glass to enhance physical-mechanical properties of fired clay brick. *J Clean Prod*. 112, 3057–3062 (2016). <https://doi.org/10.1016/j.jclepro.2015.10.084>
- [37] Hasan, M.R., Siddika, A., Akanda, M.P.A., Islam, M.R.: Effects of waste glass addition on the physical and mechanical properties of brick. *Innovative Infrastructure Solutions*. 6, (2021). <https://doi.org/10.1007/s41062-020-00401-z>
- [38] Berov, D., Klayn, S.: Microplastics and floating litter pollution in Bulgarian Black Sea coastal waters. *Mar Pollut Bull*. 156, 1–6 (2020). <https://doi.org/10.1016/j.marpolbul.2020.111225>
- [39] van der Hal, N., Ariel, A., Angel, D.L.: Exceptionally high abundances of microplastics in the oligotrophic Israeli Mediterranean coastal waters. *Mar Pollut Bull*. 116, 151–155 (2017). <https://doi.org/10.1016/j.marpolbul.2016.12.052>
- [40] Xu, P., Peng, G., Su, L., Gao, Y., Gao, L., Li, D.: Microplastic risk assessment in surface waters: A case study in the Changjiang Estuary, China. *Mar Pollut Bull*. 133, 647–654 (2018). <https://doi.org/10.1016/j.marpolbul.2018.06.020>

- [41] Nie, H., Wang, J., Xu, K., Huang, Y., Yan, M.: Microplastic pollution in water and fish samples around Nanxun Reef in Nansha Islands, South China Sea. *Science of the Total Environment*. 696, 1–7 (2019). <https://doi.org/10.1016/j.scitotenv.2019.134022>
- [42] Sarkar, D.J., Das Sarkar, S., Das, B.K., Praharaj, J.K., Mahajan, D.K., Purokait, B., Mohanty, T.R., Mohanty, D., Gogoi, P., Kumar V, S., Behera, B.K., Manna, R.K., Samanta, S.: Microplastics removal efficiency of drinking water treatment plant with pulse clarifier. *J Hazard Mater*. 413, 1–9 (2021). <https://doi.org/10.1016/j.jhazmat.2021.125347>
- [43] Reddy, S.R., Fogler, H.S.: *Emulsion Stability: Determination from Turbidity*. (1981)
- [44] Worrall, W.E.: *Clays and Ceramic Raw Materials*. Springer Netherlands, Berlin (1986)
- [45] Yakub, I., Plappally, A., Leftwich, M., Malatesta, K., Friedman, K.C., Obwoya, S., Nyongesa, F., Maiga, A.H., Asce, M., Alfred, J., Soboyejo, B.O., Logothetis, S., Soboyejo, W.: Porosity, flow, and filtration characteristics of frustum-shaped ceramic water filters. *Journal of Environmental Engineering*. 139, 986–994 (2013). [https://doi.org/10.1061/\(ASCE\)EE.1943-7870](https://doi.org/10.1061/(ASCE)EE.1943-7870)
- [46] Mouratib, R., Achiou, B., Krati, M. El, Younsi, S.A., Tahiri, S.: Low-cost ceramic membrane made from alumina- and silica-rich water treatment sludge and its application to wastewater filtration. *J Eur Ceram Soc*. 40, 5942–5950 (2020). <https://doi.org/10.1016/j.jeurceramsoc.2020.07.050>
- [47] Leriche, A., Hampshire, S., Cambier, F.: Sintering of Ceramics. In: *Reference Module in Materials Science and Materials Engineering*. pp. 1–23 (2017)
- [48] Mustapha, S., Oladejo, T.J., Muhammed, N.M., Saka, A.A., Oluwabunmi, A.A., Abdulkabir, M., Joel, O.O.: Fabrication of porous ceramic pot filters for adsorptive removal of pollutants in tannery wastewater. *Sci Afr*. 11, 1–17 (2021). <https://doi.org/10.1016/j.sciaf.2021.e00705>
- [49] Malik, N., Bulasara, V.K., Basu, S.: Preparation of novel porous ceramic microfiltration membranes from fly ash, kaolin and dolomite mixtures. *Ceram Int*. 46, 6889–6898 (2020). <https://doi.org/10.1016/j.ceramint.2019.11.184>
- [50] Kamgang-Syapnjeu, P., Njoya, D., Kamseu, E., Balme, S., Bechelany, M., Soussan, L.: Bio-based ceramic membranes for bacteria removal from water. *Membranes (Basel)*. 12, 1–11 (2022). <https://doi.org/10.3390/membranes12090901>
- [51] Cui, Z., Hao, T., Yao, S., Xu, H.: Preparation of porous mullite ceramic supports from high alumina fly ash. *J Mater Cycles Waste Manag*. 25, 1120–1129 (2023). <https://doi.org/10.1007/s10163-023-01598-8>
- [52] Vakifahmetoglu, C., Semerci, T., Soraru, G.D.: Closed porosity ceramics and glasses, (2020)
- [53] Silva, K.R., Menezes, R.R., Campos, L.F.A., Santana, L.N.L.: A review on the production of porous ceramics using organic and inorganic industrial waste. *Ceramica*. 68, 270–284 (2022). <https://doi.org/10.1590/0366-69132022683873309>
- [54] Frizon, C.N.T., Perussello, C.A., Sturion, J.A., Hoffmann-Ribani, R.: Novel beverages of yerba-mate and soy: Bioactive compounds and functional properties. *Beverages*. 4, 1–11 (2018). <https://doi.org/10.3390/beverages4010021>
- [55] Croge, C.P., Cuquel, F.L., Pintro, P.T.M.: Yerba mate: Cultivation systems, processing and chemical composition. a review. *Sci Agric*. 78, 1–11 (2020). <https://doi.org/10.1590/1678-992x-2019-0259>
- [56] Gawron-Gzella, A., Chanaj-Kaczmarek, J., Cielecka-Piontek, J.: Yerba mate - a long but current history. *Nutrients*. 13, 1–19 (2021). <https://doi.org/10.3390/nu13113706>
- [57] Heck, C.I., De Mejia, E.G.: Yerba mate tea (*Ilex paraguariensis*): A comprehensive review on chemistry, health implications, and technological considerations. *J Food Sci*. 72, R138–R151 (2007). <https://doi.org/10.1111/j.1750-3841.2007.00535.x>
- [58] Beltrame, D.M. de O., De Carvalho, P.O., Ribeiro, M.L., Helena Markowicz Bastos, D., Moura de Oliveira, D., Lobato Teixeira Matsumoto, R., de Oliveira Carvalho, P., Lima Ribeiro, M.: Yerba maté: Pharmacological Properties, Research and Biotechnology. *Med Aromat Plant Sci Biotechnol*. 1, 37–46 (2007)
- [59] Matthies, K., Bitter, H., Deobald, N., Heinle, M., Diedel, R., Obst, U., Brenner-Weiss, G.: Morphology, composition and performance of a ceramic filter for household water treatment in Indonesia. *Water Pract Technol*. 10, 361–370 (2015). <https://doi.org/10.2166/wpt.2015.044>



This article is licensed under a [Creative Commons Attribution 4.0 International License](https://creativecommons.org/licenses/by/4.0/).